RSC Advances

PAPER

View Article Online
View Journal | View Issue

Cite this: *RSC Adv.*, 2015, **5**, 65897

Electrospun nanofibers incorporating self-decomposable silica nanoparticles as carriers for controlled delivery of anticancer drug

Xiaojun Zhou,[ab] Liang Chen,[a] Weizhong Wang,[a] Yating Jia,[a] Anni Chang,[a] Xiumei Mo,[ab] Hongsheng Wang[a] and Chuanglong He*[ab]

Received 19th June 2015
Accepted 21st July 2015

DOI: 10.1039/c5ra11830a

www.rsc.org/advances

Drug delivery *via* electrospun nanofibers represents a new approach to treat tissue damage resulting from cancer or cancer treatment. In this study, we propose a decomposable nanoparticle-incorporated electrospun mat as carrier for anticancer drugs. The anticancer drug doxorubicin (DOX) was initially loaded into SiO_2 nanoparticles (DOX@SiO_2), and the prepared DOX-loaded nanoparticles were then introduced into a poly(lactic-*co*-glycolic acid)/chitosan (PLGA/CS) mixed solution to fabricate drug-loaded composite nanofibers (PLGA/CS/DOX@SiO_2) *via* electrospinning. The prepared nanoparticles and drug-loaded nanofibers were characterized by various methods, and the results indicated that the DOX@SiO_2 nanoparticles were dispersively embedded inside PLGA/CS nanofibers. The PLGA/CS/DOX@SiO_2 composite nanofibers showed a sustained and controlled drug release profile. Moreover, the DOX released from the composite nanofibers achieved significant antitumor activity, thereby effectively inhibiting the growth of HeLa cells. Thus, the prepared composite nanofibrous mats containing self-decomposable nanocarriers would be potential candidates for cancer treatment.

Introduction

Electrospinning, which was first patented by Formhals[1] early in 1934, has been demonstrated to be a simple and versatile technique to produce polymer nanofibers with diameters ranging from nanometers to several micrometers. The morphology of electrospun nanofibers can be controlled by adjusting the solution parameters, process parameters, and ambient parameters.[2] In addition, due to their attractive features such as large specific surface area, high porosity, feasibility for surface functionalization and extracellular matrix-like structure, electrospun nanofibers have been applied in many fields including tissue engineering,[2–7] wound dressing,[8] and drug delivery.[9]

Currently, cancer therapy remains a tremendous challenge due to the complexities and variability involved in cancer progression.[10,11] Patients suffering from cancer need to take excessive amounts of antitumor drugs orally or *via* systematic injection to allow the drug to be delivered to the site of the cancer, which may induce undesirable side effects in healthy tissues.[12,13] It is hence critically important that a therapeutic amount of drug is delivered to the target tumor site and effectively absorbed by the surrounding cancer cells.[14] As compared to conventional drug formulations, localized drug delivery systems offer the possibility of sustained and targeted delivery of drugs, and hence allow for improved efficacy of chemotherapy, reduced toxic side effects and decreased frequency of drug administration.[15] Recently, electrospun nanofibers have been extensively explored as new carriers for anticancer drugs, due to the main advantage of offering site-specific delivery of drugs to a site.[16–18] Furthermore, the drug release from electrospun nanofibers can be controlled by modulating the fiber composition, morphology, diameter and porosity.[19] However, when a drug is encapsulated within nanofibers by simply electrospinning of drug and polymer mixture, an undesirable burst release is frequently inevitable due to the high ionic strength in solution and the rapid evaporation of the solvent during electrospinning.[20] To overcome this, several inorganic nanocarriers have been entrapped into electrospun nanofibers in order to prevent initial burst release and provide a slow sustainable release.[21–23] For instance, we have previously reported that the anticancer drug doxorubicin (DOX) can be released in a controlled manner from mesoporous silica nanoparticle-incorporated electrospun nanofibers.[23] In such a drug delivery system, drugs were firstly loaded into nanocarriers which were then incorporated into electrospun nanofibers, resulting in a prolonged and sustained drug release.

In a previous study, Zhang *et al.*[24] reported a kind of unique drug-loaded silica nanoparticles by introducing drug molecules into the silica nanoparticles during nanoparticle growth under

[a]*College of Chemistry, Chemical Engineering and Biotechnology, State Key Laboratory for Modification of Chemical Fibers and Polymer Materials, Donghua University, Shanghai 201620, China. E-mail: hcl@dhu.edu.cn*

[b]*College of Materials Science and Engineering, Donghua University, Shanghai 201620, China*

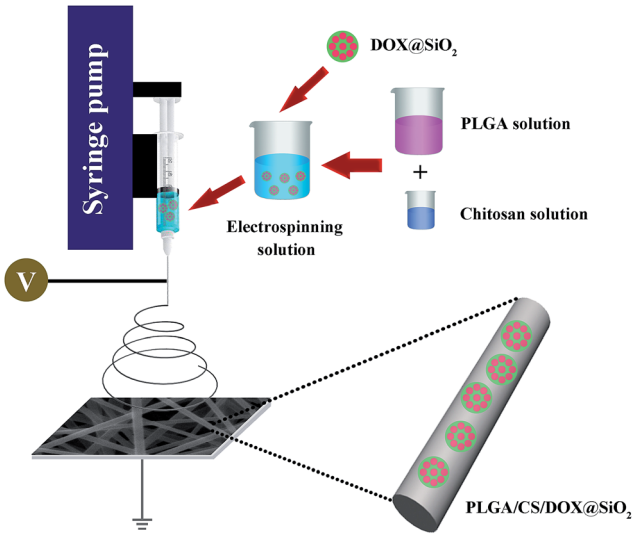

Fig. 1 Schematic illustration for the process of fabrication of PLGA/CS/DOX@SiO_2 electrospun composite nanofibers.

controlled conditions, from which the drug can be released along with the carrier decomposition. Therefore, it is desired to incorporate such decomposable drug carriers into electrospun nanofibers. Herein, we report, to the best of our knowledge, the first study to develop decomposable silica nanoparticle-embedded electrospun nanofibers for potential cancer treatment. DOX was firstly loaded into SiO_2 to form drug-loaded nanoparticles (denoted as DOX@SiO_2), and then the DOX@SiO_2 nanoparticles were combined with a poly(lactic-*co*-glycolic acid)/chitosan (PLGA/CS) mixed solution to fabricate composite nanofibrous mats (denoted as PLGA/CS/DOX@SiO_2) by electrospinning (Fig. 1). The obtained nanofibrous mats were characterized using different techniques. The drug release profiles of different DOX-containing nanofibrous mats were investigated, and the antitumor activity of the PLGA/CS/DOX@SiO_2 composite nanofibrous mats was evaluated by the MTT cytotoxicity assay on HeLa cells. Furthermore, the antitumor efficacy of this material was further investigated *via* confocal microscopic observation. Our results suggested that the developed composite nanofibrous mats may be a promising candidate for cancer therapy.

Experimental

Materials and methods

PLGA copolymers with LA/GA ratio of 75 : 25 (M_w = 110 kDa) were purchased from Jinan Daigang Biomaterials Co. Ltd (China). DOX (M_w = 580) was obtained from Beijing Huafeng United Technology Co. Ltd (Beijing, China). Chitosan (medium molecular weight, degree of deacetylation of 75–85%) and tetraethylorthosilicate (TEOS) were obtained from Sigma-Aldrich (Shanghai) Trading Co. Ltd (Shanghai, China). Dulbecco's modified Eagle's medium (DMEM), fetal bovine serum (FBS), penicillin–streptomycin, and trypsin were obtained from Gibco Life Technologies Co. (Grand Island, USA). Alexa Fluor 488 phalloidin was obtained from Invitrogen Trading Co. Ltd (Shanghai, China). 3-(4,5-Dimethylthiazol-2-yl)-2,5-diphenyltetrazoliumbromide (MTT) was obtained from Shanghai Yuanxiang Medical Equipment Co. Ltd. All other chemicals were of analytical grade, purchased from Sinopharm Chemical Reagent Co. Ltd (Shanghai, China) and used without further purification.

Preparation of DOX@SiO_2

DOX@SiO_2 nanoparticles were prepared using a facile method as reported previously with some modifications.[24,25] Briefly, 10 mg of DOX was first added into a mixture of 75 mL of ethanol with 3.4 mL of ammonia solution (25%). After stirring for 30 min, 0.08 mL of TEOS was quickly added into the mixed solution. Then the DOX@SiO_2 nanoparticles were collected by centrifugation after stirring for 24 h, and washed several times with ethanol and water. After that, the DOX@SiO_2 nanoparticles were dried under vacuum for further use. The drug loading capacity of DOX@SiO_2 was measured by dissolving DOX@SiO_2 into an aqueous solution of hydrofluoric acid and then determining the mass of free drug (2.2 mg DOX per 100 mg DOX@SiO_2) using an ultraviolet-visible (UV-vis) spectrophotometer (JASCO V-530, Japan) at a wavelength of 480 nm.[26]

Electrospinning

PLGA/CS/DOX@SiO_2 nanofibrous mats were prepared by blend electrospinning of DOX@SiO_2 nanoparticles, chitosan and PLGA. For comparison, neat PLGA/CS, PLGA/CS/DOX, and PLGA/DOX@SiO_2 nanofibrous mats were also prepared. A 20% (w/v) PLGA solution was prepared by dissolving PLGA in hexafluoroisopropanol. Chitosan was dissolved in trifluoroacetic acid to prepare a 4% (w/v) chitosan solution. After that, chitosan and PLGA solutions were mixed in a volume ratio of 1/9. Then DOX@SiO_2 nanoparticles (5 wt% relative to PLGA) were blended with the mixed solutions of PLGA and chitosan by gentle stirring for 12 h at room temperature. For electrospinning, the solution was loaded in a 5 mL syringe and injected through a stainless-steel blunt needle (inner diameter of 0.8 mm). The electrospinning process was performed with a feeding rate of 0.5 mL h^{-1} from the syringe pump, an applied voltage of 15 kV, and a distance of 15 cm between the tip of the needle and the collector. The collected nanofibrous mats were finally dried under vacuum for at least 72 h to remove the residual solvent before further use.

Characterization

The morphology and structure of DOX@SiO_2 nanoparticles were characterized using transmission electron microscopy (TEM, JEM-2100, Japan). The incorporation of DOX@SiO_2 within electrospun mats was observed using TEM. The morphology of electrospun mats was observed using a field emission scanning electron microscope (FESEM, Hitachi S-4800, Japan). The average diameter of nanofibers was obtained from at least 100 measurements of a typical FESEM image using ImageJ 1.40G software (NIH, USA). The particle size distributions and the polydispersity indices (PDI) of DOX@SiO_2 were measured by a Zetasizer Nano ZS instrument (Malvern,

UK). Attenuated total reflectance-Fourier transform infrared (ATR-FTIR) spectroscopy was conducted with a Nicolet 670 (Thermo Nicolet, USA).

In vitro drug release

The *in vitro* release profile of DOX from nanoparticles or nanofibrous mats was determined using a UV-vis spectrophotometer by measuring the maximum absorbance wavelengths at 480 nm. All the electrospun mats were cut into 2.0 × 2.0 cm^2 square pieces and their weights were accurately measured. The release behavior of DOX@SiO_2 was also evaluated as a reference. Each sample was placed into a centrifuge tube filled with 10 mL of phosphate buffered saline solution (PBS, pH 7.4). The tube was then incubated at 37 °C in a thermostatically controlled shaker with constant rotation at a speed of 100 rpm. 4 mL of release medium was extracted at predetermined time intervals for analysis and replaced with an equal volume of fresh PBS. The amount of DOX released for each sample was measured using the UV-vis spectrophotometer. The experiments were carried out in triplicate per sample.

Antitumor activity assay

HeLa cells were cultured in DMEM supplemented with 10% FBS, 100 U mL^{-1} penicillin and 100 μg mL^{-1} streptomycin in a humidified incubator with 5% CO_2 at 37 °C. The *in vitro* cell viability of PLGA/CS/DOX@SiO_2 against HeLa cells was evaluated by MTT assay. For comparison, the cytotoxicity of free DOX, DOX@SiO_2, PLGA/CS/DOX and PLGA/DOX@SiO_2 with the equivalent amount of DOX was assessed. Before cell seeding, all the samples were sterilized overnight under UV light irradiation. Briefly, HeLa cells were seeded in 24-well plates (2 × 10^4 cells per well) for 24 h to allow cell attachment. The cells were then incubated with free DOX, DOX@SiO_2, PLGA/CS/DOX, PLGA/DOX@SiO_2 and PLGA/CS/DOX@SiO_2 at the same DOX concentrations (1, 5 and 10 μg mL^{-1}). Neat PLGA/CS nanofibers with the equivalent mass corresponding to PLGA/CS/DOX were also used. After the cells were incubated for 48 h, the culture medium was removed and replaced with 360 μL fresh culture medium, followed by the addition of 40 μL MTT solution. After incubation for another 4 h, the suspension was discarded and 400 μL DMSO was added into each well to allow the purple MTT formazan crystals to dissolve. Then, 100 μL of the dissolved formazan solution was transferred into 96-well plates for testing. The OD value at 492 nm was measured using a microplate reader (MK3, Thermo, USA). The cytotoxicity was expressed as the percentage of cell viability as compared with the blank control, and the mean value was calculated from three parallel samples.

To further investigate the cytocompatibility of the prepared samples, the morphologies of HeLa cells treated with various samples (PLGA/CS, free DOX, DOX@SiO_2 and PLGA/CS/DOX@SiO_2 nanofibrous mats) were observed using confocal laser scanning microscopy (CLSM, Carl Zeiss LSM 700, Germany). Briefly, HeLa cells were seeded into 24-well plates at a density of 1 × 10^4 cells per well and incubated for 24 h. Then, the culture medium was removed and the cells were incubated with PLGA/CS, free DOX, DOX@SiO_2 and PLGA/CS/DOX@SiO_2 (DOX concentrations of 10 μg mL^{-1}) for another 48 h. After washing with PBS twice, the cells were fixed with 4% paraformaldehyde for 10 min. The cells were then permeabilized in 0.1% Triton X-100 in PBS for 5 min, followed by blocking with 1% bovine serum albumin for 20 min. The actin of cells was stained by using Alexa Fluor 488 phalloidin solution for 10 min. Finally, all samples were washed several times with PBS and observed by CLSM.

Statistical analysis

All values are presented as mean ± standard deviation. Statistical analysis was carried out by a one-way analysis of variance (one-way ANOVA) and Scheffe's *post hoc* test. The criteria for statistical significance were $*P < 0.05$ and $**P < 0.01$.

Results and discussion

Characterization of DOX@SiO_2

The morphology and structure of DOX@SiO_2 nanoparticles were characterized by TEM. As shown in Fig. 2A, they were spherical in shape and with no pore structure within the particles. The hydrodynamic size of DOX@SiO_2 was 122.7 nm, with a PDI of 0.102, suggesting uniform nanoparticles (Fig. 2B). As DOX was incorporated into the nanoparticles in the synthetic process, the absorption spectra of samples were used to determine the successful incorporation. Comparing with the pure DOX absorption measured in aqueous solution, its characteristic absorption at ~480 nm was clearly observed in the spectrum of the DOX@SiO_2 sample (Fig. 2C). Additionally, the inset in Fig. 2C shows a digital image of DOX@SiO_2 suspended in aqueous solution with a light red color, which also indicated that DOX was successfully incorporated into SiO_2 particles.

TEM images were acquired to examine the morphological evolution of the DOX@SiO_2 nanoparticles after immersion in

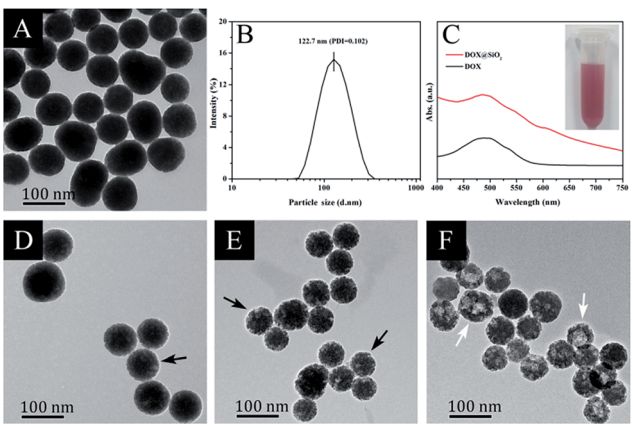

Fig. 2 Characterization of DOX@SiO_2 nanoparticles. (A) TEM image of DOX@SiO_2. (B) Size distribution curve of DOX@SiO_2. (C) Absorption spectra taken from DOX@SiO_2 and pure DOX in aqueous solutions. Inset image is a DOX@SiO_2 suspension (5 mg mL^{-1}). TEM images of DOX@SiO_2 after being immersed in deionized water at 37 °C for (D) 2, (E) 4 and (F) 10 days.

deionized water at 37 °C for different time periods. As depicted in Fig. 2D–F, most of the nanoparticles remained intact at day 2, but slight damage was observed on the outer surface. After 4 days immersion, obvious decomposition was observed at the outer surface of the nanoparticles (marked by black arrows in Fig. 2E). At day 10, a hollow feature occurred in the center of the nanoparticles (marked by white arrows in Fig. 2F). Hence, we considered that the DOX@SiO_2 nanoparticles would continue to be damaged and eventually decomposed into scattered fragments in the following days, coinciding with the result of a previous report.[24] Based on the above experimental results, a possible mechanism could be proposed. In the early time, DOX molecules in the outer surface were first released, which drove the collapse of outer silica. It was reasonable that the silica structure in the center of the nanoparticles was the most vulnerable as they were mainly composed of high-concentration DOX with little silica components. After longer time of immersion, some of the DOX molecules were moved out from the center of nanoparticles, which caused the collapse of central SiO_2 (as they grow together with the DOX during DOX@SiO_2 nanoparticle formation). As a result, the nanoparticles were totally damaged when all DOX molecules were released and subsequent silica decomposition. Therefore, this self-decomposable carrier was beneficial for elimination from biologic systems.

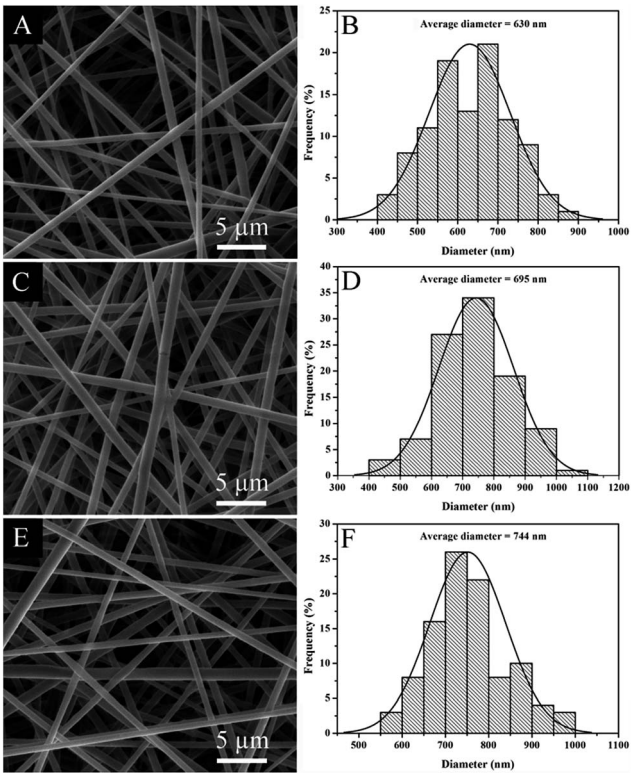

Fig. 3 SEM images and diameter distribution histograms of (A and B) neat PLGA nanofibers, (C and D) neat PLGA/CS nanofibers, and (E and F) PLGA/CS/DOX@SiO_2 composite nanofibers.

Preparation and characterization of electrospun nanofibers

The DOX@SiO_2 nanoparticles were incorporated into PLGA/CS nanofibers *via* electrospinning to form PLGA/CS/DOX@SiO_2 composite nanofibers (Fig. 1). Neat PLGA and PLGA/CS nanofibers were also prepared in the same manner and used as controls. The morphologies of the nanofibers were characterized by SEM. Fig. 3 shows the morphology and diameter distribution of nanofibers. It can be seen that the surface of the PLGA and PLGA/CS nanofibers was smooth, and no beads were observed on the surface (Fig. 3A and C). Even after DOX@SiO_2 incorporation, the composite nanofibers were still smooth and beadless, with no nanoparticles being seen on the surface of the nanofibers (Fig. 3E). The average diameters of PLGA, PLGA/CS and PLGA/CS/DOX@SiO_2 nanofibers were 630, 695 and 744 nm, respectively (Fig. 3B, D and F). The diameter increase of PLGA/CS nanofibers could result from the addition of chitosan, which enhanced the viscosity of the composite solution.[27,28] In addition, the greater average diameter of PLGA/CS/DOX@SiO_2 nanofibers may be due to the increase in viscosity of the electrospun solution after the addition of DOX@SiO_2 nanoparticles.[23,29,30]

Fig. 4A shows the FTIR spectra of the electrospun PLGA, PLGA/CS and PLGA/CS/DOX@SiO_2 nanofibers. For these samples, the strong characteristic absorption band at 1756 cm^{-1} can be attributed to the stretching vibration of C=O bond of PLGA,[31] while the weak peak appearing at 1672 cm^{-1} in the spectra of PLGA/CS and PLGA/CS/DOX@SiO_2 nanofibers was assigned to the amide I absorption band of chitosan.[27] However, no characteristic absorption peaks of DOX@SiO_2 can be observed in the spectrum of PLGA/CS/DOX@SiO_2 nanofibers (detailed data not shown), which may be because DOX@SiO_2 was effectively embedded into the interior of the composite nanofibers.

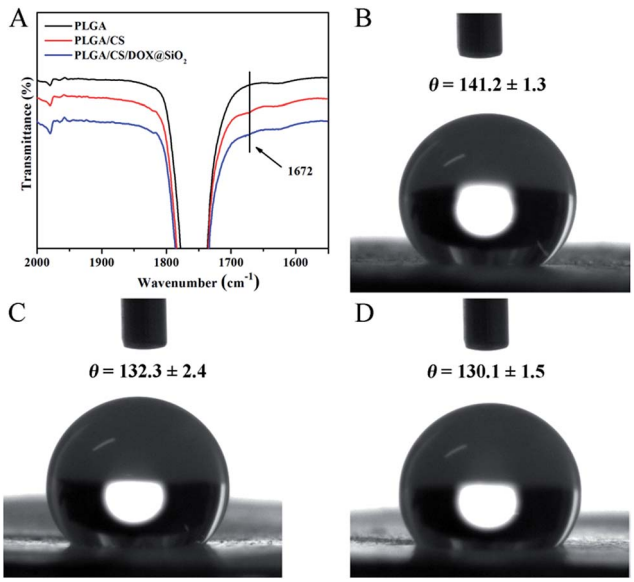

Fig. 4 (A) FTIR spectra of electrospun nanofibers. Water contact angle of electrospun nanofibers: (B) neat PLGA nanofibers, (C) PLGA/CS nanofibers, and (D) PLGA/CS/DOX@SiO_2 composite nanofibers.

The surface hydrophilicity plays an important role in the practical application of electrospun nanofibers. Fig. 4B–D indicates the water contact angles of different nanofibrous mats after water droplets were placed on the surface. It can be seen that the water contact angle of PLGA/CS was 132.3° (Fig. 4C), which was slightly less than that of the pure PLGA because of the presence of a small amount of chitosan (2.2 wt% relative to PLGA). Thus, the hydrophilicity of nanofibrous mats can be enhanced by the addition of chitosan. Furthermore, the addition of DOX@SiO_2 (5 wt% relative to PLGA) did not significantly change the hydrophilicity of PLGA/CS/DOX@SiO_2 nanofibrous mats (Fig. 4D).

TEM and fluorescence microscopy were used to confirm the incorporation of the DOX@SiO_2 nanoparticles into the composite nanofibers (Fig. 5). Compared to the pure nanofibers, the spherical DOX@SiO_2 nanoparticles within the composite nanofibers with uniform distribution can be clearly observed (Fig. 5A and B). The TEM image in Fig. 5B indicates that DOX@SiO_2 nanoparticles were successfully embedded in the nanofibers. The DOX loaded in the nanofibers can be observed *via* the red fluorescence of DOX using fluorescence microscopy (Fig. 5C and D). Similar to the DOX-loaded PLGA/CS nanofibers, the red fluorescence of DOX can be clearly observed in the PLGA/CS/DOX@SiO_2 nanofibers. Meanwhile, only a few small red fluorescence spots caused by the partial aggregation of nanoparticles were present in the image of the nanofibers. This result further revealed that the DOX@SiO_2 nanoparticles can be embedded in PLGA/CS nanofibers with uniform distribution within the nanofibers.

Release of DOX from the nanofibrous mats

The *in vitro* release of DOX from the electrospun mats was studied by exposure of the nanofibrous mats in PBS solution (pH = 7.4) at 37 °C. For comparison, the release of DOX from DOX@SiO_2 nanoparticles, PLGA/CS/DOX and PLGA/DOX@SiO_2 nanofibrous mats was also investigated. Fig. 6 shows the release profiles of DOX from the different samples. All the electrospun mats showed a gradual increase in DOX release with increasing time. The release of DOX from both DOX@SiO_2 nanoparticles and PLGA/CS/DOX nanofibrous mats was significantly faster than that from the PLGA/DOX@SiO_2 and PLGA/CS/DOX@SiO_2 nanofibrous mats. This result was mainly because DOX can directly move out from the SiO_2 and PLGA/CS matrix. For those samples, furthermore, a burst release appeared during the first 24 h, with more than 25% of DOX released for both samples. For PLGA/CS/DOX@SiO_2 sample, the release of DOX showed a moderate rate within 24 h, with 15.3% of DOX released. Then, the subsequent release of DOX followed a sustained release, with the total amount of DOX released being about 58% after 369 h. In contrast, although DOX release from PLGA/DOX@SiO_2 was of a sustained manner, the release rate was significantly slow, with only 33.6% of DOX released at 369 h.

For both PLGA/DOX@SiO_2 and PLGA/CS/DOX@SiO_2 nanofibrous mats, the DOX release rates were slower and the maximum amounts of DOX released were less than for other samples, which can be explained in that DOX tends to be first released from the SiO_2 matrix, and subsequently released from the PLGA or PLGA/CS matrix to the medium. In addition, the release rate of DOX from PLGA/CS/DOX@SiO_2 was faster than that from PLGA/DOX@SiO_2. In general, a smaller fiber diameter results in faster drug release since a fiber with smaller diameter has a larger specific surface area, and thus allows good water penetration and exposure.[32] In this study, the average fiber diameter could be increased by the addition of chitosan. In contrast, the DOX release rate of PLGA/CS/DOX@SiO_2 was relatively fast, which can be attributed to the addition of chitosan resulting in a greater swelling of the nanofibers, and thus allowing DOX molecules to diffuse from the matrix into the medium more easily.[33] Thus, DOX release from PLGA/CS/

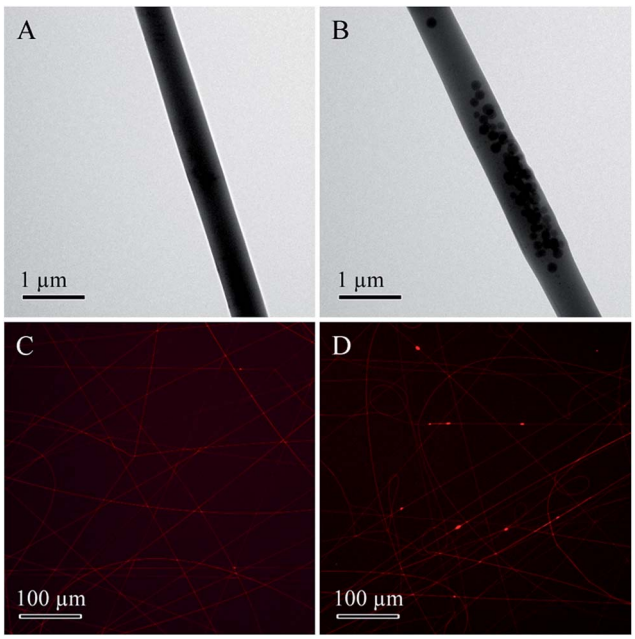

Fig. 5 TEM images of (A) neat PLGA/CS nanofiber and (B) PLGA/CS/DOX@SiO_2 composite nanofiber. Fluorescence images of (C) PLGA/CS/DOX nanofibers and (D) PLGA/CS/DOX@SiO_2 composite nanofibers.

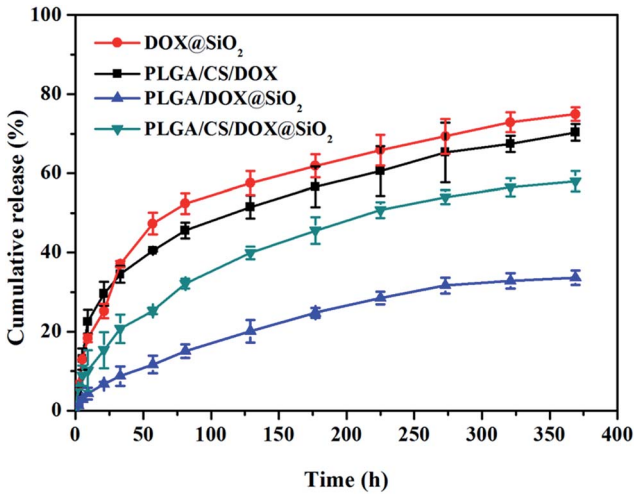

Fig. 6 *In vitro* release of DOX from DOX@SiO_2 nanoparticles and PLGA/CS/DOX, PLGA/DOX@SiO_2 and PLGA/CS/DOX@SiO_2 composite nanofibers.

$DOX@SiO_2$ was characterized by a sustained release profile and a more appropriate release rate. This drug release behavior is preferable for the inhibition of tumor cell growth by providing sufficient concentration of anticancer drug over the therapeutic period.

Antitumor activity assay

For the antitumor application of drug-containing materials, it is essential to investigate the antitumor activity of the drug released from the matrices. The *in vitro* cytotoxicity of the nanofibers against HeLa cells was evaluated by MTT assay. Fig. 7 presents the cell viability of HeLa cells treated with different samples with DOX concentrations ranging from 1 to 10 μg mL^{-1} for 48 h incubation. It is clear that the neat PLGA/CS nanofibers did not show any obvious cytotoxicity to HeLa cells within the tested concentrations. But for other samples (free DOX, $DOX@SiO_2$ nanoparticles, $PLGA/DOX@SiO_2$, PLGA/CS/DOX and $PLGA/CS/DOX@SiO_2$ nanofibers), the cytotoxicity of them against HeLa cells increased with an increase of the DOX concentration. The free DOX displayed a statistically significantly higher inhibition effect than other samples within the measured concentrations ($P < 0.01$). This is probably due to the direct contact between DOX and cells and initial high concentration of DOX. At DOX concentrations of 5 and 10 μg mL^{-1}, the cytotoxicity of $PLGA/DOX@SiO_2$ was lower than that of $DOX@SiO_2$ nanoparticles, PLGA/CS/DOX nanofibers and $PLGA/CS/DOX@SiO_2$ nanofibers, which was attributed to the slow release rate of DOX from the nanofibers. It is noted that there were no statistically significant differences among $DOX@SiO_2$ nanoparticles, PLGA/CS/DOX and $PLGA/CS/DOX@SiO_2$ nanofibers at a DOX concentration of 10 μg mL^{-1} for cytotoxicity against HeLa cells, with cell viability of 30.9%, 33.5% and 35.2%, respectively. This result indicated that $DOX@SiO_2$ nanoparticles incorporated into PLGA/CS nanofibers can effectively inhibit the growth of HeLa cells. Although the antitumor efficacy of $PLGA/CS/DOX@SiO_2$ nanofibers cannot reach the performance of the pure DOX in a short time, a long-term growth inhibition in cancer cells resulting from the sustained DOX release was expected, which was beneficial for *in vivo* therapeutic effect.

To further confirm the antitumor activity of the prepared composite nanofibers, we next observed the morphological changes of HeLa cells treated with different samples at a DOX concentration of 10 μg mL^{-1} by using CLSM. Fig. 8 shows the CLSM images of HeLa cells which were incubated with different samples for 48 h. The green fluorescence represents the signal from actin stained using Alexa Fluor 488 phalloidin, and the red fluorescence indicates the DOX. It was observed that the morphology of HeLa cells was intact and extended after treatment with PLGA/CS nanofibers, which was similar to the control group, suggesting that there was no toxic effect of the PLGA/CS sample under the conditions of this study. However, HeLa cells treated with free DOX, $DOX@SiO_2$ nanoparticles and

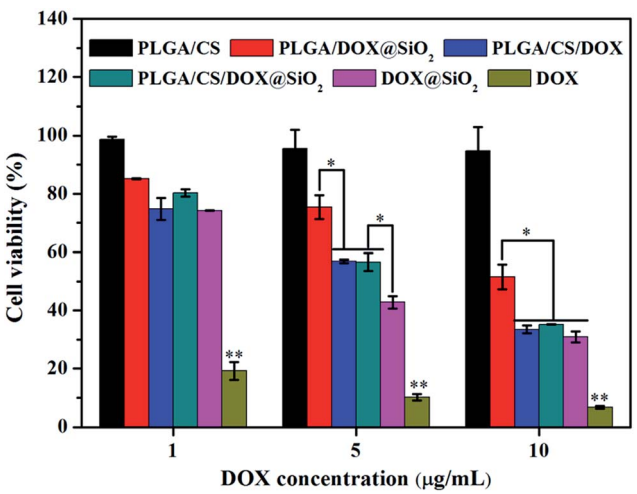

Fig. 7 The cell viability of HeLa cells treated with various samples with DOX concentrations ranging from 1 to 10 mg mL^{-1} for 48 h. **Significant difference compared to other groups ($P < 0.01$).

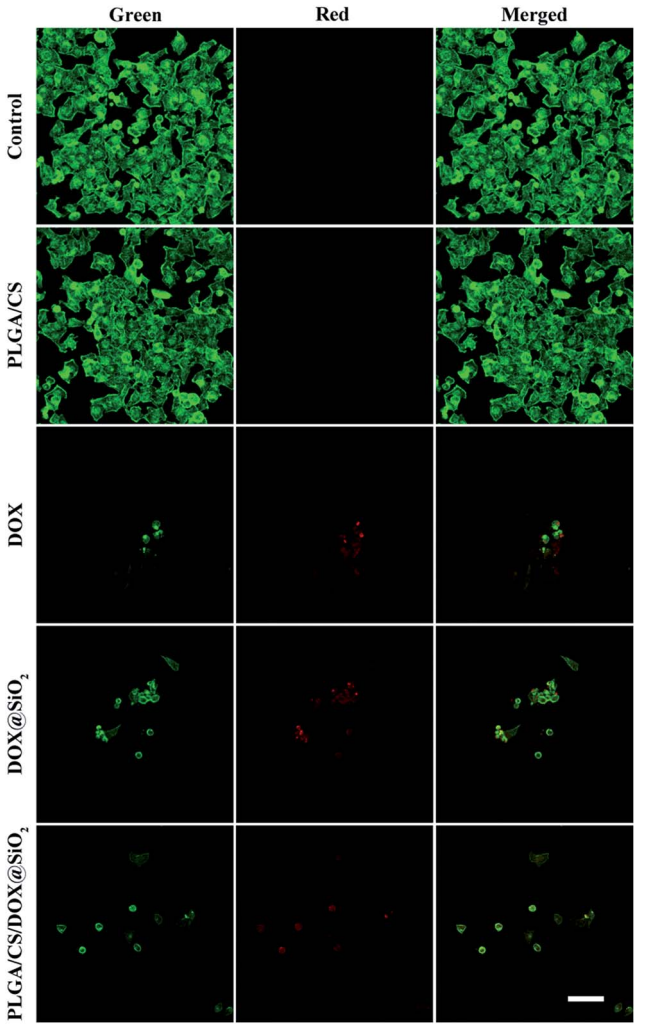

Fig. 8 Confocal laser scanning microscopy images of HeLa cells treated with different samples for 48 h. DOX concentration was 10 μg mL^{-1}. The red fluorescence represents the released DOX. The green fluorescence represents Alexa Fluor 488 phalloidin-stained F-actin. Scale bar = 100 μm.

PLGA/CS/DOX@SiO_2 nanofibers displayed apoptotic morphological changes with reduced cell number and round-shaped morphology. Additionally, we noted that the cytotoxicity of PLGA/CS/DOX@SiO_2 nanofibers was similar to that of DOX@SiO_2 nanoparticles and weaker than that of free DOX, which was consistent with the result of MTT assays. The obvious antitumor activity of PLGA/CS/DOX@SiO_2 sample indicated that the released DOX can effectively inhibit the growth of cancer cells. Based on these results, we can expect that the decomposable DOX@SiO_2-embedded electrospun composite nanofibers would maintain efficient and long-term antitumor efficacy, which might be used for future cancer treatment.

As a potential novel drug delivery carrier, silica nanoparticles can be incorporated into electrospun nanofibers to achieve sustained and controlled drug release from the resultant composite matrices.[30] For example, mesoporous silica nanoparticles have been proposed as effective drug carriers to be embedded into electrospun nanofibers for sustained release of an encapsulated drug.[23,30] In this work, decomposable SiO_2 nanoparticles were used as drug carriers, which provide a special benefit for attaining the desired drug release profile simply by tuning the drug diffusion and silica decomposition. Therefore, the designed PLGA/CS/DOX@SiO_2 composite nanofibrous mat is effective for drug release and is easily eliminated from biologic systems after decomposition, which make it suitable as a potential implantable drug delivery system for preventing cancer recurrence.

Conclusions

In this study, PLGA/CS/DOX@SiO_2 composite nanofibers with smooth surface morphology were successfully fabricated by electrospinning. The incorporated DOX@SiO_2 nanoparticles could self-decompose with the release of DOX molecules. After the addition of chitosan, the average diameter of the resultant composite nanofibers increased and the water contact angle was slightly enhanced. Thus, we found that DOX was released from PLGA/CS/DOX@SiO_2 composite nanofibers at a moderate release rate and in a sustained release manner, which is beneficial for biomedical applications requiring the drug to maintain long-term antitumor efficacy. Furthermore, the results of MTT assay and CLSM images confirm that the DOX released from the PLGA/CS/DOX@SiO_2 composite nanofibers can effectively inhibit the growth of HeLa cells. Therefore, the prepared PLGA/CS/DOX@SiO_2 nanofibrous mat can provide sustained release of anticancer drugs, which is highly desirable for application in cancer therapy.

Acknowledgements

This study was financially supported by the National Natural Science Foundation of China (31271028), Innovation Program of Shanghai Municipal Education Commission (13ZZ051), Open Foundation of State Key Laboratory for Modification of Chemical Fibers and Polymer Materials (LK1416) and Chinese Universities Scientific Fund (CUSF-DH-D-2014019).

Notes and references

1 F. Anton, Process and apparatus for preparing artificial threads, US Pat., 1975504, 1934.
2 C. He, W. Nie and W. Feng, *J. Mater. Chem. B*, 2014, **2**, 7828.
3 W. J. Li, C. T. Laurencin, E. J. Caterson, R. S. Tuan and F. K. Ko, *J. Biomed. Mater. Res.*, 2002, **60**, 613.
4 C. He, X. Jin and P. X. Ma, *Acta Biomater.*, 2014, **10**, 419.
5 C. He, G. Xiao, X. Jin, C. Sun and P. X. Ma, *Adv. Funct. Mater.*, 2010, **20**, 3568.
6 W. J. Yang, J. Fu, D. X. Wang, T. Wang, H. Wang, S. G. Jin and N. Y. He, *J. Biomed. Nanotechnol.*, 2010, **6**, 254.
7 T. Wang, X. Y. Ji, L. Jin, Z. Q. Feng, J. H. Wu, J. Zheng, H. Y. Wang, Z. W. Xu, L. L. Guo and N. Y. He, *ACS Appl. Mater. Interfaces*, 2013, **5**, 3757.
8 Z. X. Cai, X. M. Mo, K. H. Zhang, L. P. Fan, A. L. Yin, C. L. He and H. S. Wang, *Int. J. Mol. Sci.*, 2010, **11**, 3529.
9 H. Jiang, Y. Hu, Y. Li, P. Zhao, K. Zhu and W. Chen, *J. Controlled Release*, 2005, **108**, 237.
10 W. Feng, X. Zhou, W. Nie, L. Chen, K. Qiu, Y. Zhang and C. He, *ACS Appl. Mater. Interfaces*, 2015, **7**, 4354.
11 M. Cao, X. R. Liu, J. B. Tang, M. H. Sui and Y. Q. Shen, *Sci. China: Chem.*, 2014, **57**, 633.
12 M. Zamani, M. P. Prabhakaran and S. Ramakrishna, *Int. J. Nanomed.*, 2013, **8**, 2997.
13 S. Y. Zhang, Y. Wu, B. He, K. Luo and Z. W. Gu, *Sci. China: Chem.*, 2014, **57**, 461.
14 X. Xu, X. Chen, Z. Wang and X. Jing, *Eur. J. Pharm. Biopharm.*, 2009, **72**, 18.
15 K. E. Uhrich, S. M. Cannizzaro, R. S. Langer and K. M. Shakesheff, *Chem. Rev.*, 1999, **99**, 3181.
16 S. T. Yohe, V. L. Herrera, Y. L. Colson and M. W. Grinstaff, *J. Controlled Release*, 2012, **162**, 92.
17 S. H. Ranganath and C.-H. Wang, *Biomaterials*, 2008, **29**, 2996.
18 X. L. Xu, X. S. Chen, X. Y. Xu, T. C. Lu, X. Wang, L. X. Yang and X. B. Jing, *J. Controlled Release*, 2006, **114**, 307.
19 S. Wang, Y. Zhao, M. Shen and X. Shi, *Ther. Delivery*, 2012, **3**, 1155.
20 C. L. He, Z. M. Huang and X. J. Han, *J. Biomed. Mater. Res., Part A*, 2009, **89**, 80.
21 F. Zheng, S. Wang, S. Wen, M. Shen, M. Zhu and X. Shi, *Biomaterials*, 2013, **34**, 1402.
22 M. Chen, W. Feng, S. Lin, C. He, Y. Gao and H. Wang, *RSC Adv.*, 2014, **4**, 53344.
23 K. Qiu, C. He, W. Feng, W. Wang, X. Zhou, Z. Yin, L. Chen, H. Wang and X. Mo, *J. Mater. Chem. B*, 2013, **1**, 4601.
24 S. Zhang, Z. Chu, C. Yin, C. Zhang, G. Lin and Q. Li, *J. Am. Chem. Soc.*, 2013, **135**, 5709.
25 D. B. Tada, L. L. Vono, E. L. Duarte, R. Itri, P. K. Kiyohara, M. S. Baptista and L. M. Rossi, *Langmuir*, 2007, **23**, 8194.
26 Q. He, Y. Gao, L. Zhang, Z. Zhang, F. Gao, X. Ji, Y. Li and J. Shi, *Biomaterials*, 2011, **32**, 7711.

27 Z. Meng, W. Zheng, L. Li and Y. Zheng, *Mater. Chem. Phys.*, 2011, **125**, 606.
28 X. Y. Ji, W. J. Yang, T. Wang, C. Mao, L. L. Guo, J. Q. Xiao and N. Y. He, *J. Biomed. Nanotechnol.*, 2013, **9**, 1672.
29 M. Kanehata, B. Ding and S. Shiratori, *Nanotechnology*, 2007, **18**, 315602.
30 B. Song, C. Wu and J. Chang, *Acta Biomater.*, 2012, **8**, 1901.
31 M. V. Jose, V. Thomas, D. R. Dean and E. Nyairo, *Polymer*, 2009, **50**, 3778.
32 W. G. Cui, X. H. Li, X. L. Zhu, G. Yu, S. B. Zhou and J. Weng, *Biomacromolecules*, 2006, **7**, 1623.
33 F. L. Mi, S. S. Shyu, Y. M. Lin, Y. B. Wu, C. K. Peng and Y. H. Tsai, *Biomaterials*, 2003, **24**, 5023.